

Alma Mater Studiorum Università di Bologna  
Archivio istituzionale della ricerca

Historic Barrel Vaults Undergoing Differential Settlements

This is the final peer-reviewed author's accepted manuscript (postprint) of the following publication:

*Published Version:*

D'Altri, A.M., De Miranda, S., Castellazzi, G., Sarhosis, V., Hudson, J., Theodossopoulos, D. (2020). Historic Barrel Vaults Undergoing Differential Settlements. INTERNATIONAL JOURNAL OF ARCHITECTURAL HERITAGE, 14(8), 1196-1209 [10.1080/15583058.2019.1596332].

*Availability:*

This version is available at: <https://hdl.handle.net/11585/711915> since: 2020-04-08

*Published:*

DOI: <http://doi.org/10.1080/15583058.2019.1596332>

*Terms of use:*

Some rights reserved. The terms and conditions for the reuse of this version of the manuscript are specified in the publishing policy. For all terms of use and more information see the publisher's website.

This item was downloaded from IRIS Università di Bologna (<https://cris.unibo.it/>).  
When citing, please refer to the published version.

(Article begins on next page)

This is an Accepted Manuscript of an article published by Taylor & Francis in International Journal of Architectural Heritage on 03 Apr 2019

Available online:  
<http://www.tandfonline.com/10.1080/15583058.2019.1596332>

© 2019. This manuscript version is made available under the Creative Commons Attribution-NonCommercial-NoDerivs (CC BY-NC-ND) 4.0 International License

(<http://creativecommons.org/licenses/by-nc-nd/4.0/>)

# Historic barrel vaults undergoing differential settlements

Antonio Maria D’Altri<sup>1\*</sup>, Stefano de Miranda<sup>1</sup>, Giovanni Castellazzi<sup>1</sup>, Vasilis Sarhosis<sup>2</sup>, Jamie Hudson<sup>3</sup>,  
Dimitris Theodossopoulos<sup>4</sup>

<sup>1</sup> Department of Civil, Chemical, Environmental, and Materials Engineering (DICAM), University of Bologna, Viale del Risorgimento 2, Bologna 40136, Italy

<sup>2</sup> School of Engineering, Newcastle University, Newcastle upon Tyne, NE1 7RU, UK

<sup>3</sup> Wiss, Janney, and Elstner Associates. Pittsburgh, PA, USA

<sup>4</sup> Edinburgh School of Architecture and Landscape Architecture, University of Edinburgh, 20 Chambers Street EH1 1JZ, Edinburgh, UK

\*corresponding author: [am.daltri@unibo.it](mailto:am.daltri@unibo.it)

## ABSTRACT

A principal reason of damage in historic masonry vaults consists in relative displacements of the vaults’ abutments. Excluding the case of seismic-induced damage, cracks are often produced by differential settlements generated by the lateral wall instability or soil degradation (e.g. due to stress concentrations, non-uniform soil stratigraphy, flooding phenomena etc.). When dealing with historic vaults, the effects of long-term deformation processes cannot often be linked directly to causes, which may also be unknown. In this paper, the effects of differential settlements on historic masonry barrel vaults are investigated. An efficient 3D contact-based model was developed to reproduce experiments on a scaled pointed barrel vault (representative of a typology of late-medieval barrel vaults in Scotland) under non-uniform differential settlement. Firstly, the numerical model is used to simulate the experimental campaign, achieving good agreement in terms of crack pattern (longitudinal shear) and transverse-longitudinal deformation profiles. Then, further analyses are carried out to gain insight on the effects of several plausible uniform and non-uniform settlement patterns on representative historic barrel vaults. Various settlement configurations were analysed and complex failure patterns observed. This study could help analysts in understanding the nature of on-going deformation process in historic masonry vaults and engineers in the design of strengthening strategies.

**Keywords:** Barrel vaults; Experiment; Numerical model; Masonry; Differential settlement

## 1 Introduction

Masonry vaults have been an efficient and fire-proof roofing method in pre-modern structures, reaching a wide variety of configurations that may not always be easy to understand in terms of performance and safety. The study of simple barrel vaults can provide a base for the understanding of load paths under various support conditions, letting insight to be built for more complex forms (cross vaults, net vaults etc). Gothic barrel vaults in particular are formed by the extrusion of an arch (generatrix) along a linear distance (directrix). As with any arch based construction, the vault produces an outward thrust along its edge and there are several mechanisms for absorbing this thrust. One is to make the wall exceedingly thick or add buttresses. Alternatively, a more elegant method is to build two or more vaults parallel to each other, cancelling mutually the forces of their outward thrust. However, the amount of thrust also depends on the shape of the arch. For example, in [1], Romano and Ochsendorf showed that pointed vaults generate significantly smaller lateral thrust to their support than semi-circular ones and thus this shape can be used to build higher and more slender walls. Furthermore, pointed arches can span larger distance with the same structural thickness. By decreasing the lateral thrust at the wall, larger windows can be built to allow for more light in the building.

Although a lot of thought and wisdom has been put into the design of arches and vaults, unfortunately, today, most of the existing historic masonry vaults stand in a damaged (cracked) condition. The main reasons of such damage arise from aging of material, soil subsidence, support failure due to poor foundations. Earthquakes can also induce significant damage to masonry vaults [2], as the oscillations can produce relative displacements between the vaults' abutments [3]. In general, although masonry vaults have great strength to vertical uniform loads, their capability to withstand differential settlements of the abutments is extremely low. Differential settlements can derive from masonry material or soil degradation (e.g. due to stress concentrations, non-uniform soil stratigraphy, etc.). However, the challenge faced during structural inspection is that although the effects of an on-going process of deformation are clear (visible cracks) on the vault, the nature and origin of the on-going settlement may remain unknown to the surveyor.

Today, several tools are available for the structural analysis of vaults and can be categorised in three main groups: (i) limit analysis-based approaches; (ii) continuum-based approaches; and (iii) block-based approaches. Limit analysis-based approaches can follow the lower bound (static approach [4, 5, 6, 7, 8, 9]) or the upper bound (kinematic approach [10, 11]) theorems of limit analysis. To apply limit analysis to masonry, three main assumptions are generally made: a) masonry has no tensile strength; b) masonry has infinite strength in compression; and c) no sliding can occur between the blocks. These approaches are considerably effective to evaluate the stability of vaults and domes. However, their capability to analyse vaults undergoing differential settlements is still under investigation. Continuum-based approaches consider masonry as a homogeneous material in which the constitutive law is described in a phenomenological way [3, 12, 13, 14]. These approaches can support any kind of boundary conditions at the vault's abutments. However, the reliability of continuum constitutive laws for historic masonry vaults is still under study. Finally, block-based approaches consider the structure as an assembly of separate blocks which can interact through specific laws. This approach represents the most accurate analysis tool [15, 16, 17, 18, 19, 20, 21, 22], even if the description of a historic vault block-by-block is still challenging and computationally demanding. In this framework, software tools based on limit analysis of rigid blocks have been lately developed for the 2D analysis of masonry bridges (LimitState: RING software originally developed in [23]), and for the limit analysis of masonry structures modelled as assemblages of 3D rigid blocks subjected to live loads and settlements (LiABlock\_3D [24]). Very recently, part of the authors developed an effective damaging block-based model for the monotonic [25] and cyclic [26] analysis of masonry panels and full-scale terraced houses.

In this paper, the effects of differential settlements on historic masonry barrel vaults are investigated. An efficient 3D non-standard contact-based distinct blocks model, based on the advances presented in [25, 26], is implemented to reproduce experiments on a scaled pointed barrel vault specimen (representative of late medieval barrel vaults from Scotland), under non-uniform differential settlement. The choice of Scottish vaults is because they follow a specific typology during 15<sup>th</sup> century and they are plain yet very well built. Firstly, the numerical model is used to simulate the experimental campaign. The numerical results validate the

experiments in terms of crack pattern and transverse-longitudinal deformation profiles. This makes possible further analyses to gain an insight on the effects of several plausible uniform and non-uniform settlement patterns on a representative historic barrel vault. Various settlement patterns were simulated and the complex failure mode of the vault investigated. This study could help analysts in understanding the nature of on-going deformation processes in historic masonry vaults and consequently in assisting engineers in the design of strengthening strategies.

As final note, it has to be pointed out that full-scale tests on actual historic masonry vaults are very rare due to heritage protection and specialist equipment and happen mainly during repairs, i.e. monitoring only specific aspects of the project. Scale models are usually utilized for the qualitative understanding of the structural response of masonry vaults, as the experimental set-up considered in this paper had aimed to do for Gothic barrel vaults undergoing non-uniform settlements, without precise quantitative conclusions. This experimental test has been found to be appealing as it dealt with the simple geometry of barrel vaults, avoiding the complex conditions along intersections at groin vaults or the oversimplification of an arch. Moreover, the test interpreted reasonably well the real deformation of an existing vault (Bothwell) under differential settlement [27]. This made easier the evaluation of the potential of a block-based modelling approach in vaults. Indeed, as typically expected from computational tools, if the numerical results are found to be consistent with the experimental outcomes of the test on a scale model, it is reasonable to assume that the numerical approach can be used for quantitative predictions on full-scale actual masonry vaults as well.

## **2 Scottish gothic vaults**

Barrel vaults in collegiate (private) churches in late-medieval Scotland (15<sup>th</sup> century) are a quite well-defined group in terms of their character, design and structural scheme (Fig. 1), so they are a comprehensive typology and case study. They may have origins in secular architecture, especially castles and tower-houses [28], where usually their spatial articulation and decoration (ribs) would denote higher status, but strength and fire-proofing were equally attractive. When applied to single volume churches though, the scheme does not borrow the solid envelope that contained the thrust very effectively there but relies on buttresses to let windows, which usually open below springing level, so the geometry of the barrel is not disturbed. Their geometric study [29, 30] shows pointed profiles largely generated within an equilateral triangle. Parallel ribs divide them into bays and often mask construction breaks (as was found during the repair works in Bothwell in 2014-16, Fig. 1a). Consequently, there is no roof truss above them and flagstones cover the vault, laid directly on a rubble fill on the extrados or possibly diaphragm walls (called *frenelli* in Italy), adding a substantial load on the vault.



Fig. 1 – The earliest (a) (Bothwell 1398) and latest (b) (Ladykirk 1500) examples of barrel vaults in late-medieval Scotland churches. Crack pattern in Bothwell (c) due to deformation in the South wall from [27] and its appearance at the East end of the interior (following repairs in 2016), (settlement caused at the right-hand corner).

Considering the construction evolution since the earliest (1398) to the latest (1500) examples, we can observe that pier buttresses contain the thrust and become thicker and safer towards the end of the period (e.g. Ladykirk, Fig. 1b). Construction also improves in its visual expression, using polished ashlar (Crichton in 1449, Seton in 1478). Measured surveys [29] have shown precision in the execution of the form and very little deformation. This was not the case of the Bothwell church though (Fig. 1a), which has suffered differential settlement on its South side (Fig. 1c), as the foundations had slipped outwards and the clay under the south-east corner had settled significantly, and had to undergo repair and bracing (2014-16). The horizontal spread component of this vault was examined first [30] in an experimental and analytical programme of a homogeneous model and then the vertical settlement only in a masonry-replica model [27], showing the vulnerability of the scheme to such instability. The two damage patterns were quite similar as well, which makes repair to a certain extent easier to plan.

### 3 Experimental tests

An attempt was made to construct a representative in geometry model of the barrel vault in the quire (choir) of Bothwell. A measured survey of the vault was carried out by the church once realised its geometry was slightly skewed and cracks started opening due to settlement over the years across the less braced South edge. A 1/12 scale was chosen for the construction of the model in the laboratory as it was convenient for the shaping of the blocks and the experimental set-up. To focus on the study of the original form of the Bothwell barrel



vault, its shape was kept simple and symmetric. This resulted in a model of an interior span equal to 508 mm and a rise of 317 mm, keeping the length of the vault as 1,400 mm. Particularly, the physical model was characterized by a thickness of about 30 mm. The original geometry of the Bothwell vault was based on an equilateral triangle, with the span equal to the two other sides of the section of the barrel vault. The same characteristic has been kept in the physical model, with an inner radius of the arch equal to 405 mm. The vault was composed of a series of equal in size varnished wooden units, bonded by a lime-based mortar. The length of the wooden blocks scaled a representative block of the original vault and the height to width ratio was  $2/3$ . Mortar was composed of 3 parts of sand and 1 part of lime. Then, PVA glue and water were added. This mixture was used in previous experiments involving cross vaults [31] and it has been found to be convenient for construction reasons [27].

The model vault was subjected to a vertical displacement of one of the corners producing a linear displacement along its edge (Fig. 2a). The right side of the vault was fixed while the left back corner was pinned so that the rest of the left side of the vault could rotate freely, following displacement imposed at the left front corner. Such experimental procedure has been designed to represent asymmetric differential settlement which often occurs in such structures. The vault was subjected to asymmetric settlement until collapse, which occurred at displacement of the left-hand corner of 132 mm or 42% of the rise of the vault.

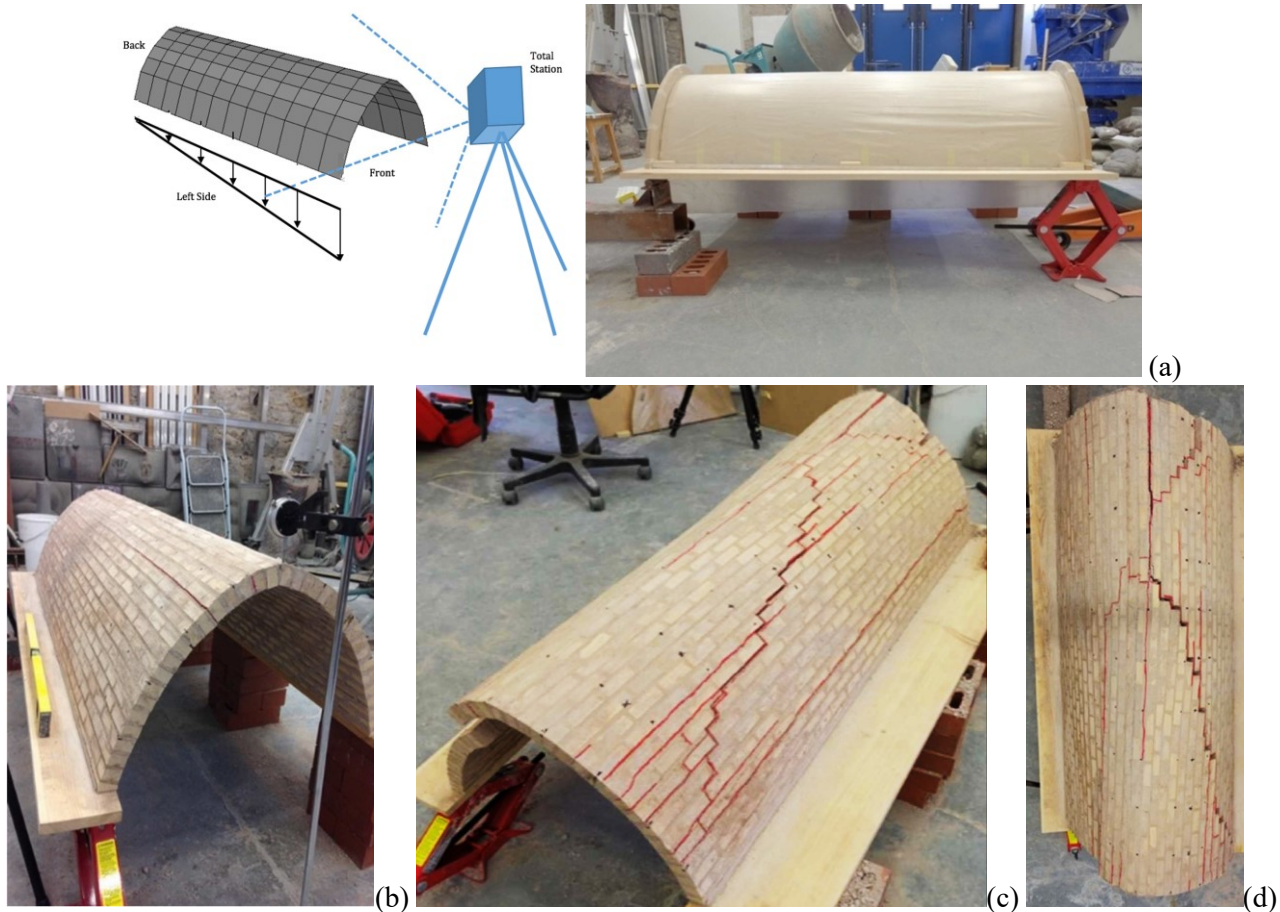


Fig. 2 – Experimental set-up (a) and cracks observed in the experiment: initial cracks (b) and crack pattern at the end of the test - corner view (c) and top view (d) [27].

During testing, a crack appeared after a settlement of 30 mm spreading longitudinally from the left front edge of the vault (Fig. 2b) and in the next stages the crack propagated quickly until the mid-span of the vault. At a settlement of 45 mm, the section of the vault along the crack began to separate and deflect visibly, while a diagonal shear crack began to form at the intrados, starting from the back-right edge and spreading at roughly

45 degrees angle towards the apex. This was accompanied by a crack along the apex spreading longitudinally from the back edge of the vault. At a settlement of 75 mm, the two cracks met, forming a hinge at the apex with the resulting triangular portion of the vault detaching from the lower vault structure. The test was continued until full collapse of the structure. Several small longitudinal cracks developed from the front of the vault near the apex. As the vault approached full collapse, a crack formed on the front extrados of the vault of the right side near the springing and propagated down the entire length, forming a hinge. In addition, another diagonal crack formed beginning at the front of the vault at 45 degrees angle. This joined with a longitudinal crack on the extrados and progressed to meet the first diagonal crack at the apex. Fig. 2c-d show the diagonal crack just before the vault collapsed.



#### 4 Numerical strategy and verification

The modelling approach adopted for the analysis of barrel vaults consists of a block-based model in which the interaction between adjacent blocks is formulated in a contact-based framework accounting for cohesion and friction, and the blocks are modelled through solid FEs (Fig. 3). The model is implemented in the general-purpose FE software Abaqus [32] using an implicit solver.

The adopted contact formulation conceives contact pairs composed of one slave face and one master face, following the traditional node-against-surface approach [33]. In particular, the nodes of the slave face contact the surface of the master face (Fig. 3a). The cohesive contact behaviour is governed by an ad-hoc modification of the standard surface-based contact behaviour available in Abaqus [32]. This contact-based cohesive behaviour has been presented by the Authors in [25] and extended to the cyclic regime in [26] for masonry walls and piers. The model has shown a good efficiency [25] with respect to other block-based models.

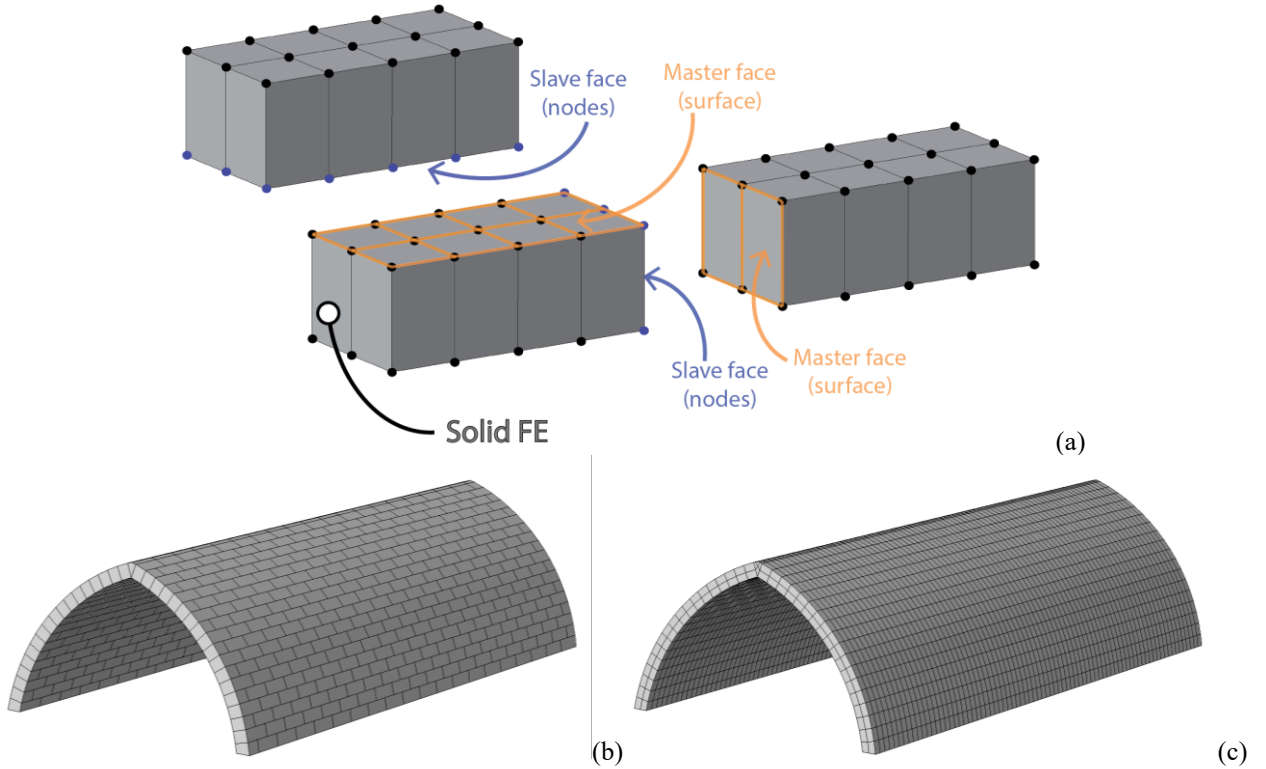


Fig. 3 – Contact-based distinct block model: node-against-surface approach (a), assembly of the blocks (b) and adopted mesh (c).

The compressive contact stress is computed by means of a Lagrange multiplier contact approach (contact constraint). Conversely, the tensile stress and the shear stress are computed, in the pre-failure regime, through the linear relationships:

$$\sigma = \begin{cases} K_{nn}u, & \sigma \geq 0 \\ \text{contact constraint}, & \sigma < 0 \end{cases}, \quad \tau = K_{ss}\delta \quad (1)$$

where  $\sigma$  is the normal contact stress (positive in tension),  $\tau$  is the shear stress,  $u$  is the normal displacement (separation),  $\delta$  is the tangential slip,  $K_{nn}$  is the cohesive stiffness in normal direction and  $K_{ss}$  is the cohesive stiffness in shear.

Contact failure is supposed when the contact stresses at a point intersects a Mohr-Coulomb failure surface with tension cut-off. This criterion can be expressed as:

$$\max \left\{ \frac{\langle \sigma \rangle}{f_t}, \frac{|\tau|}{f_s(\sigma)} \right\} = 1, \quad (2)$$

where  $\langle x \rangle = (|x| + x)/2$  means that a purely compressive stress state does not induce contact failure,  $f_t$  is the tensile strength and  $f_s$  is the shear strength defined as:

$$f_s(\sigma) = -\tan \phi \sigma + c, \quad (3)$$

where  $c$  is the cohesion and  $\tan \phi$  is the initial friction of the shear response.

The maximum normal and shear stress in a contact point are described by the relationships:

$$\sigma = \begin{cases} (1-D)f_t, & u < u_k \\ 0, & u \geq u_k \end{cases} \quad \tau = \begin{cases} (1-D)f_s(\sigma) + D\mu\langle -\sigma \rangle, & \delta < \delta_k \\ \mu\langle -\sigma \rangle, & \delta \geq \delta_k \end{cases} \quad (4)$$

where the degradation scalar variable  $D$  is defined as:

$$D = \max \left\{ \begin{aligned} &1 - \frac{u_0}{u_{MAX}} \left( 1 - \frac{1 - e^{-\zeta \frac{u_{MAX} - u_0}{u_k - u_0}}}{1 - e^{-\zeta}} \right) \\ &1 - \frac{\delta_0}{\delta_{MAX}} \left( 1 - \frac{1 - e^{-\xi \frac{\delta_{MAX} - \delta_0}{\delta_k - \delta_0}}}{1 - e^{-\xi}} \right) \end{aligned} \right\}, \quad (5)$$

being  $\mu$  the residual friction,  $u_0$  and  $\delta_0$  the separation and the slip at the limit of the linear elastic behaviour in tension and shear, respectively,  $u_{MAX}$  and  $\delta_{MAX}$  the maximum separation and the maximum slip ever experienced by the contact point, respectively,  $u_k$  and  $\delta_k$  the ultimate separation and the ultimate slip of the cohesive behaviour, respectively,  $\zeta$  and  $\xi$  non-dimensional brittleness parameters in tension and shear, respectively. The cohesive behaviour in tension and shear (Fig. 4) is governed by the same degradation scalar variable  $D$ .

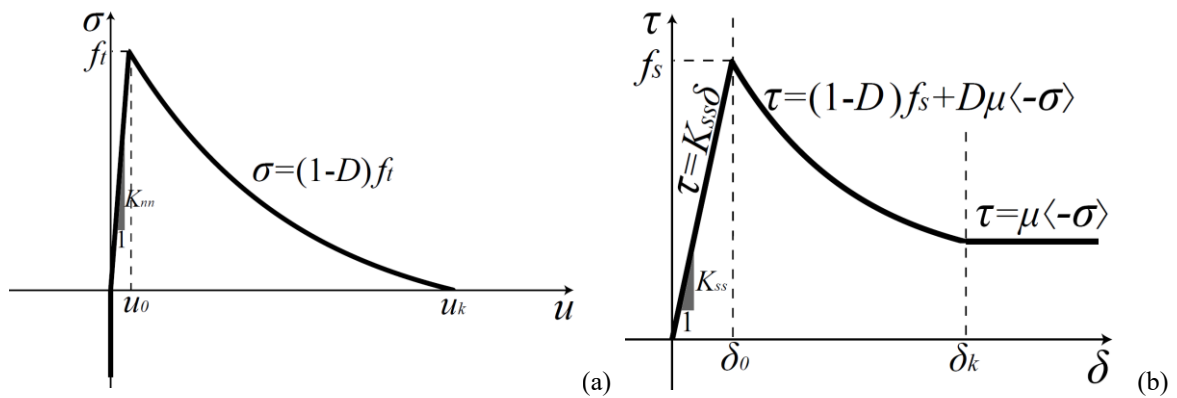


Fig. 4 – Normal (a) and shear (b) contact behaviour.

The experimental test described in Section 3 is modelled through the numerical approach here presented. The assembly of the blocks used to model the gothic barrel vault is shown in Fig. 3b and the adopted mesh (which has been found by the Authors a good compromise between accuracy and computational effort [25, 26]) is shown in Fig. 3c.

The block-based model herein adopted concerns expanded blocks (which account for the mortar layer thickness as well) assembled by zero-thickness contact-based interfaces. Therefore, mortar layers are not explicitly modelled in this numerical approach, similarly to other well-known modelling strategies [34]. However, the vault's key was realized in the physical model through a thick wedge-shaped mortar layer, see Fig. 2b. This geometric feature could not be finely represented by the numerical model, given the assumption at the basis of the modelling approach (i.e. any mortar layer explicitly modelled). Therefore, an approximation on the geometry of the vault's key was needed, and fictitious wedge-shaped blocks in the key stone were conceived.

In general, the model can be characterized by a nonlinear plastic-damage behaviour of the block, as pursued in [25, 26] to reproduce the response of brick. However, since in this case the experimental set-up was made by timber blocks, for simplicity the blocks have been described by means of an isotropic linear elastic material law, adopting the values 520 kg/m<sup>3</sup>, 9 GPa and 0.25 for density, Young's modulus and Poisson's coefficient, respectively. Since the experimental campaign [27] did not investigate the mechanical response of mortar joints, the mechanical characterization of the contact behaviour has been primarily carried out using the parameters calibrated in [25, 26] from small-scale tests. In particular, three different settings (S1, S2 and S3) of the main mechanical parameters, i.e.  $f_t$  in tension and  $c$  in shear, have been considered by keeping constant the ratio  $f_t/c = 1.5$ , which appears quite a common value as per [35]. In particular, the values of  $f_t$  and  $c$  in S2, which seem rather realistic, have been reduced four times (S1) and increased five times (S3) to realize their influence in the global structural response. The mechanical parameters used in the numerical simulations are collected in Table 1.

Given that no mechanical characterization was available for the mortar used in the experiments, the linear elastic material properties adopted for the blocks have been also used for the wedge-shaped blocks in the key stone, for simplicity. However, other preliminary analyses were performed, by using typical values of mortar Young's modulus from the literature, showing a negligible influence of this aspect on the mechanical response of the vault.

The model in Fig. 3c, after the application of the gravity load, had a non-uniform vertical settlement imposed on its left side, following the scheme depicted in Fig. 2a. The settlement has been incrementally applied to the base nodes of one side of the vault, while clamped boundary conditions have been considered for the nodes of the other side of the vault. Basically, the constraints adopted in the model attempted to follow those of the experimental test, which had no diaphragms on either end (arches) and no dead load was applied in the test during the settlement (apart from the vault's own weight). It has to be pointed out that the vault under study, on which a non-uniform vertical displacement is applied on one side, is mainly subjected to shear deformations. Therefore, the Heyman's hypotheses (high or infinite compressive strength, no tensile strength, no sliding) appear *a priori* not particularly suitable to investigate the mechanics of this vault. Indeed, by neglecting the tensile cohesion between blocks, using quasi-rigid blocks and a no sliding condition between the blocks, the vault could stand without deformations also if a single support is applied on one external edge of one abutment (while keeping the other abutment with clamped boundary conditions).

The node displacements at the extrados of the front (see Fig. 2a for reference) end of the vault, as well as the apex displacements of the whole vault, have been recorded and compared with the experimental data (Fig. 5). In particular, Fig. 5 compares the experimental and numerical deformation of the front end and the apex vertical displacement at three subsequent vertical settlements (i.e. 45mm, 75mm and 132mm) showing a reasonable agreement. In particular, the three different parameter settings (S1, S2 and S3) show slight differences, suggesting that the absolute values of tensile strength and cohesion of the interfaces do not considerably influence the failure mode and the crack pattern of the vault subjected to differential settlements, giving robustness to the adopted modelling approach.

The numerical crack pattern at the end of simulation S2 (vertical settlement equal to 132 mm) is shown in Fig. 6. Some deviations from the actual crack pattern (Fig. 2) can be noted. For example, on the left of the apex, where the experimental test shows a fast-developing detachment [27] while in the numerical model this failure is smoother and results suggest the generation of a hinge (Fig. 5). The large curvatures at width 0.2m in Fig. 5

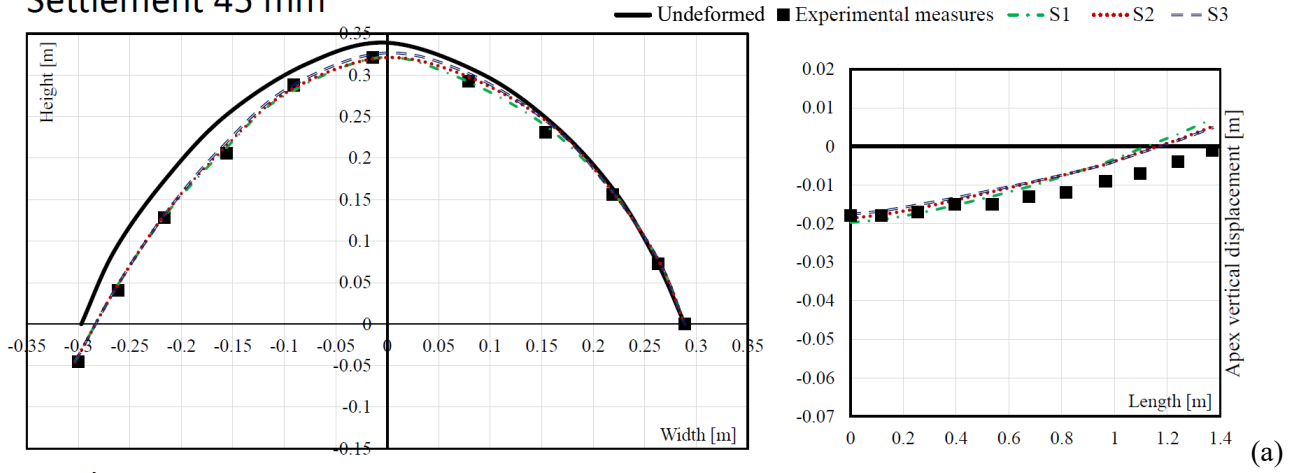
(bottom left) and the crack pattern of Fig. 6a are representative of a hinge that opens at the centre of the right midspan of the vault. Although this crack opens also in the experimental test, its magnitude seems to be slightly overestimated by the numerical analysis as the experimental measures of Fig. 5 (bottom left) and the computed displacements do not perfectly overlap on this part of the vault. Furthermore, the great relative displacement between the fourth and fifth experimental measures of Fig. 5 (bottom left) is not fully captured by the numerical model. Also, in all of the simulation, upwards vertical displacements of the apex are recorded in the sections close to the back end of the vault (Fig. 5), while the experimental profile shows upwards displacement only for large settlements (e.g. 132 mm). To this regard, it has to be pointed out that the experimental recording of displacements by means of the total station (Fig. 2a) was challenging or impossible for the points close to the back end of the vault due to the set-up. However, all things considered, the numerical results can be considered reasonably consistent with the experimental ones.

Finally, it has to be pointed out that, on the one hand, the contact properties (in terms of shear cohesion and tensile strength) do not have significant effects on the failure model of the vault (i.e. when displacements are imposed to the model). On the other hand, the influence of contact properties on the mechanical response of masonry structures (e.g. in terms of global strength) has been highlighted in other studies (see, for example, [26]).

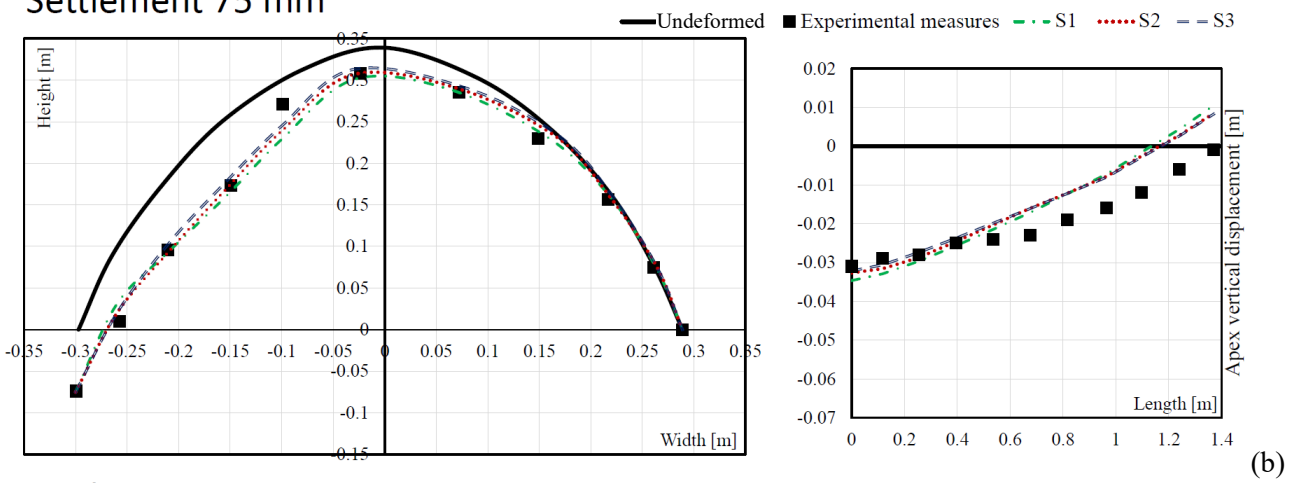
Table 1. Mechanical parameters used in the numerical simulations. When more than one value is given in a cell, the first value refers to the simulation S1, the second to S2 and the third to S3.

Tensile behaviour		Shear behaviour	
$f_t$ [MPa]	0.0075, 0.03, 0.15	$c$ [MPa]	0.005, 0.02, 0.1
$u_k$ [mm]	1.0	$\tan \phi$ [°]	0.5
$\zeta$ [°]	8	$\delta_k$ [mm]	1.0
$K_{nn}$ [N/m <sup>3</sup> ]	$75 \cdot 10^9$	$\xi$ [°]	4
		$\mu$ [°]	0.5
		$K_{ss}$ [N/m <sup>3</sup> ]	$7.5 \cdot 10^9$

### Settlement 45 mm



### Settlement 75 mm



### Settlement 132 mm

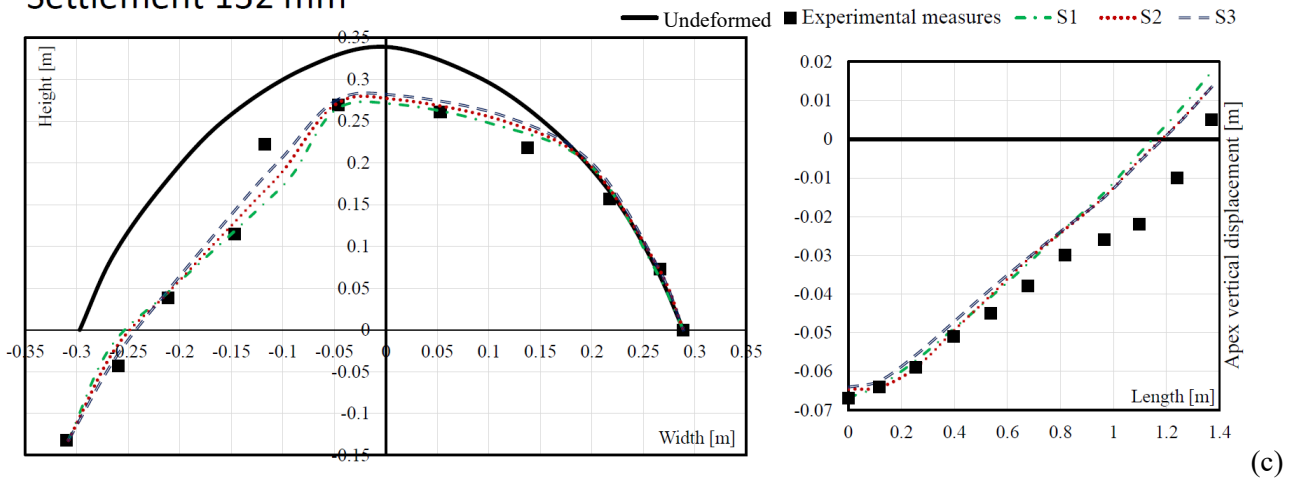


Fig. 5 – Comparison between experimental and numerical deformation of the front end (left) and apex vertical displacement (right) at three subsequent vertical settlements: (a) 45mm, (b) 75mm and (c) 132mm.

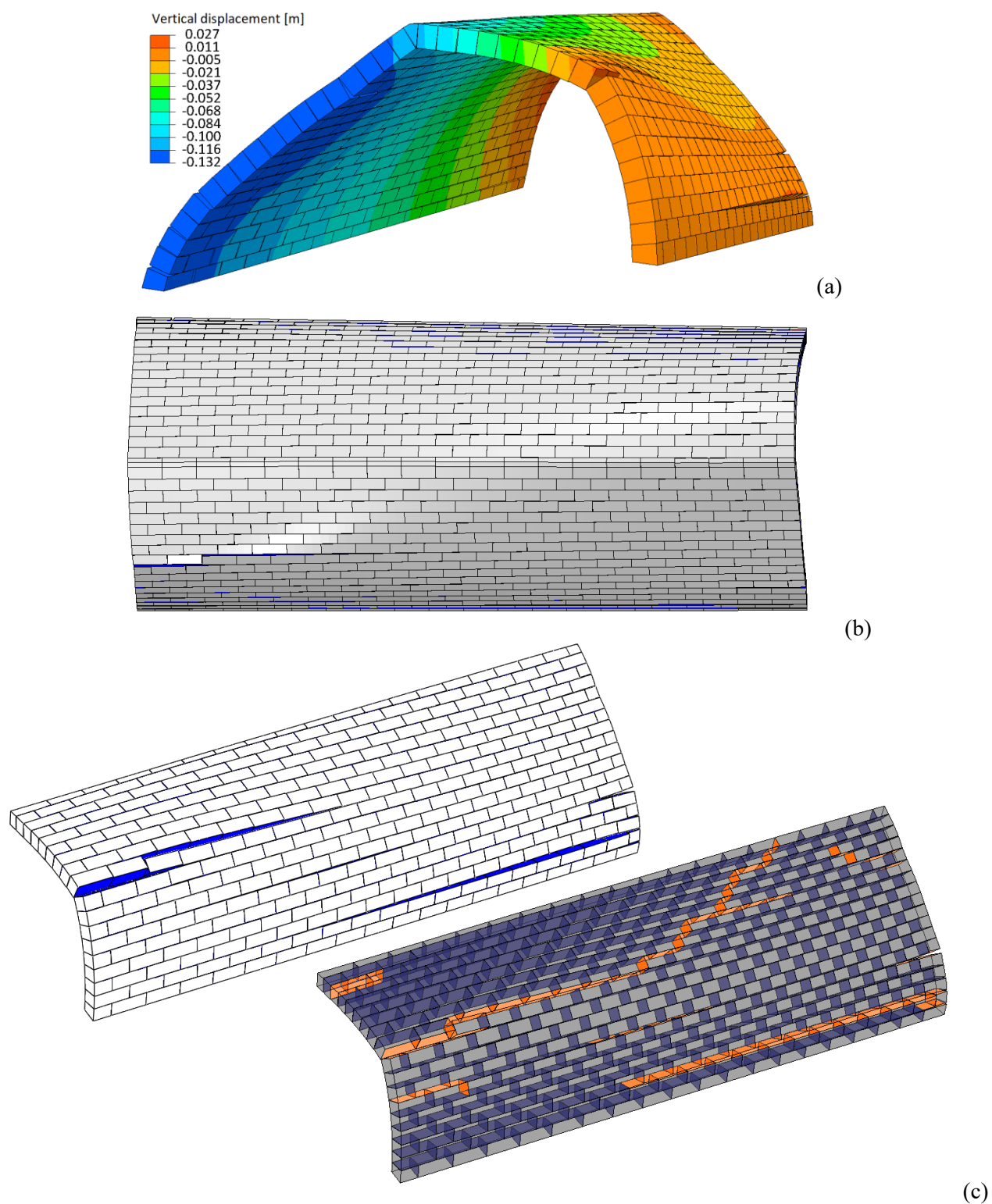


Fig. 6 – Numerical crack pattern at the end of simulation S2: vertical displacement contour plot (a), main failures in a top view (b) and interfaces which exhibited failure of the vault side opposite to the settlement (c).

## 5 Further insights on historic barrel vaults undergoing differential settlements

Further analyses were carried out to gain insight on the effects of several plausible uniform and non-uniform settlement patterns on a representative historic barrel vault model. In particular, vertical, horizontal, diagonal, inward and outward settlements are considered. The representative mechanical setting S2 has been adopted in all the analyses. The failure modes are summarized in Fig. 7 (uniform settlements) and Fig. 8 (non-uniform settlements) according to the imposed settlement pattern (left column in Fig. 7 and Fig. 8).

In general, the failure modes of uniform settlements (Fig. 7) could be also suitably predicted by an arch model, as, in this case, the bonding of the structure along the longitudinal axis plays a marginal role. Conversely, the masonry bonding plays a fundamental role in non-uniform settlements, leading to complex crack patterns (Fig. 8).

As expected, uniform horizontal settlements (outward and inward, Fig. 7) lead to symmetric crack patterns. In particular, diffuse longitudinal cracks are recorded in the extrados close to the abutments and in the intrados close to the apex for an outward settlement. Quite the opposite is recorded for an inward settlement. More localized cracks are observed in the other cases (Fig. 7 and Fig. 8).

As can be noted in Fig. 8, the failure modes of non-uniform vertical, outward horizontal and outward diagonal settlements are quite similar. On the one hand, this pools the effects of these settlements and simplifies the detection, as the exactness on the origin of the settlement is less required. On the other hand, however, an accurate knowledge on the active settlement appears more complicated as these three settlements have similar effects.

Different failure modes are, instead, observed for non-uniform inward horizontal and inward diagonal settlements Fig. 8. Indeed, although they are both characterized by an inward horizontal component of the settlement, the non-uniform inward diagonal settlement shows a crack in the extrados of the fixed side, while the non-uniform horizontal settlement shows a crack in the extrados of the active side.

Obviously, the described scenario could be further enriched by analysing other cases with different settlements and/or by considering also more complex boundary conditions to account for the effect of adjacent structural elements. By way of example, the presence of a diaphragm wall along the back end of the vault could be simulated by adopting, for simplicity, clamped boundary conditions in the nodes on the back side (Fig. 9). The crack pattern of the analysis with fixed back non-uniform vertical settlement is depicted in Fig. 9. As can be noted, although quite similar to the crack pattern of the non-uniform vertical settlement simulation (Fig. 8), several cracks arise close to the clamped side. In particular, this outcome was not visible in the non-uniform vertical settlement (Fig. 8), suggesting that the effect of a diaphragm wall on the damage pattern of a vault could result in cracks in the proximity of the diaphragm wall (Fig. 9). A similar damage pattern was observed in Bothwell (Fig. 1c) in the West side close to the West diaphragm wall, indicating a complex and sensible interaction of the vault with adjacent vertical structures.



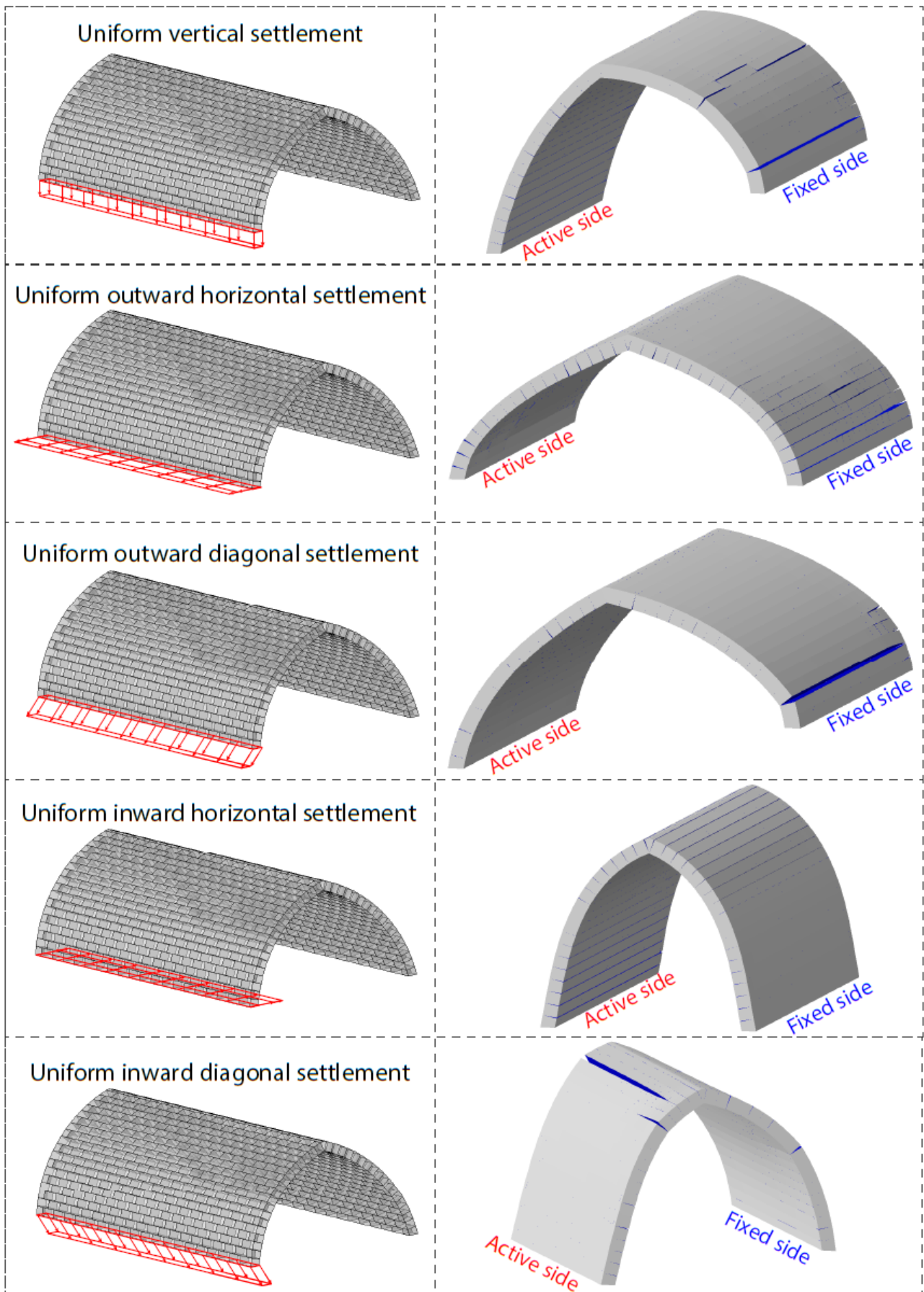


Fig. 7 – Summary of crack patterns for uniform settlements.

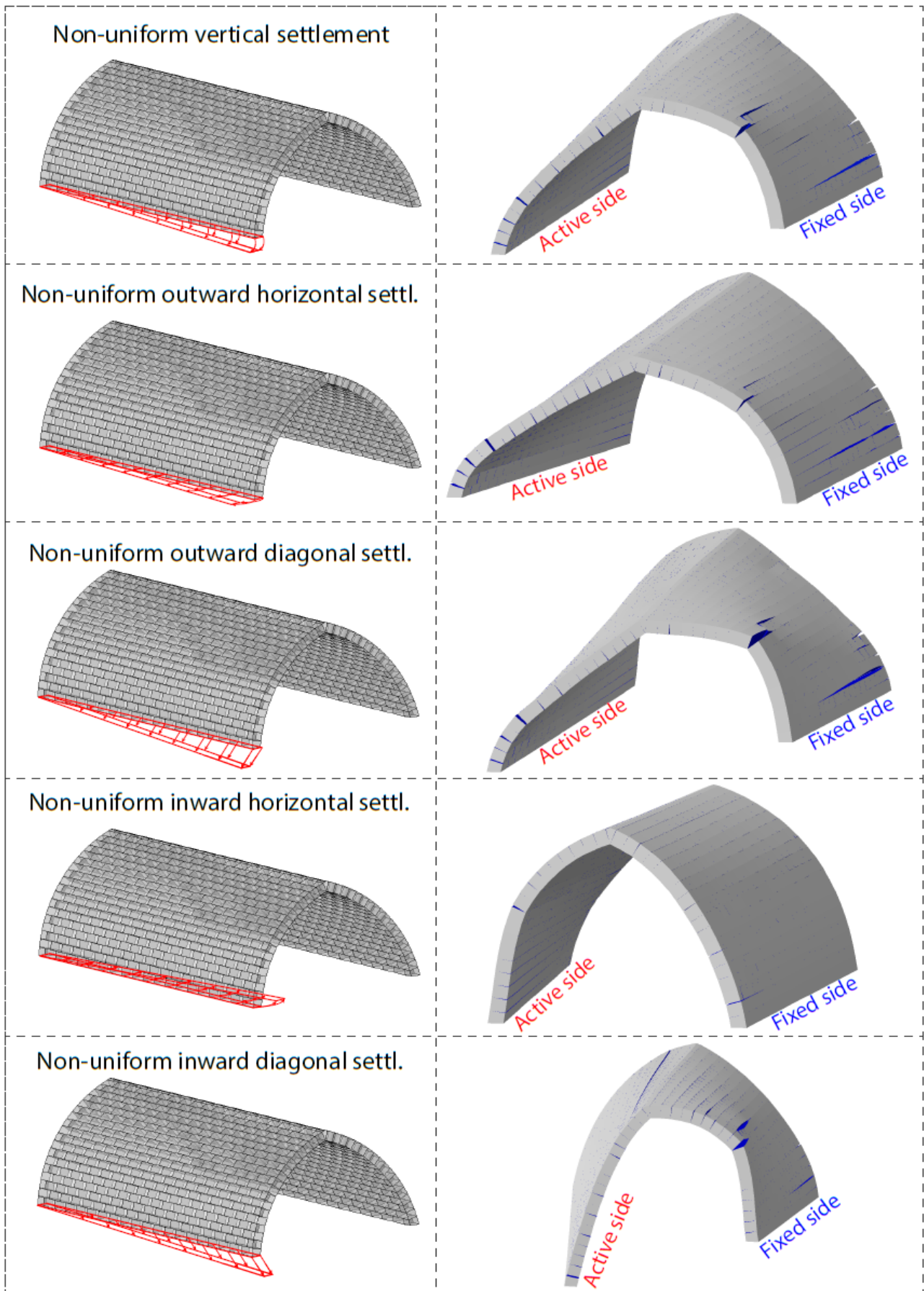


Fig. 8 – Summary of crack patterns for non-uniform settlements.

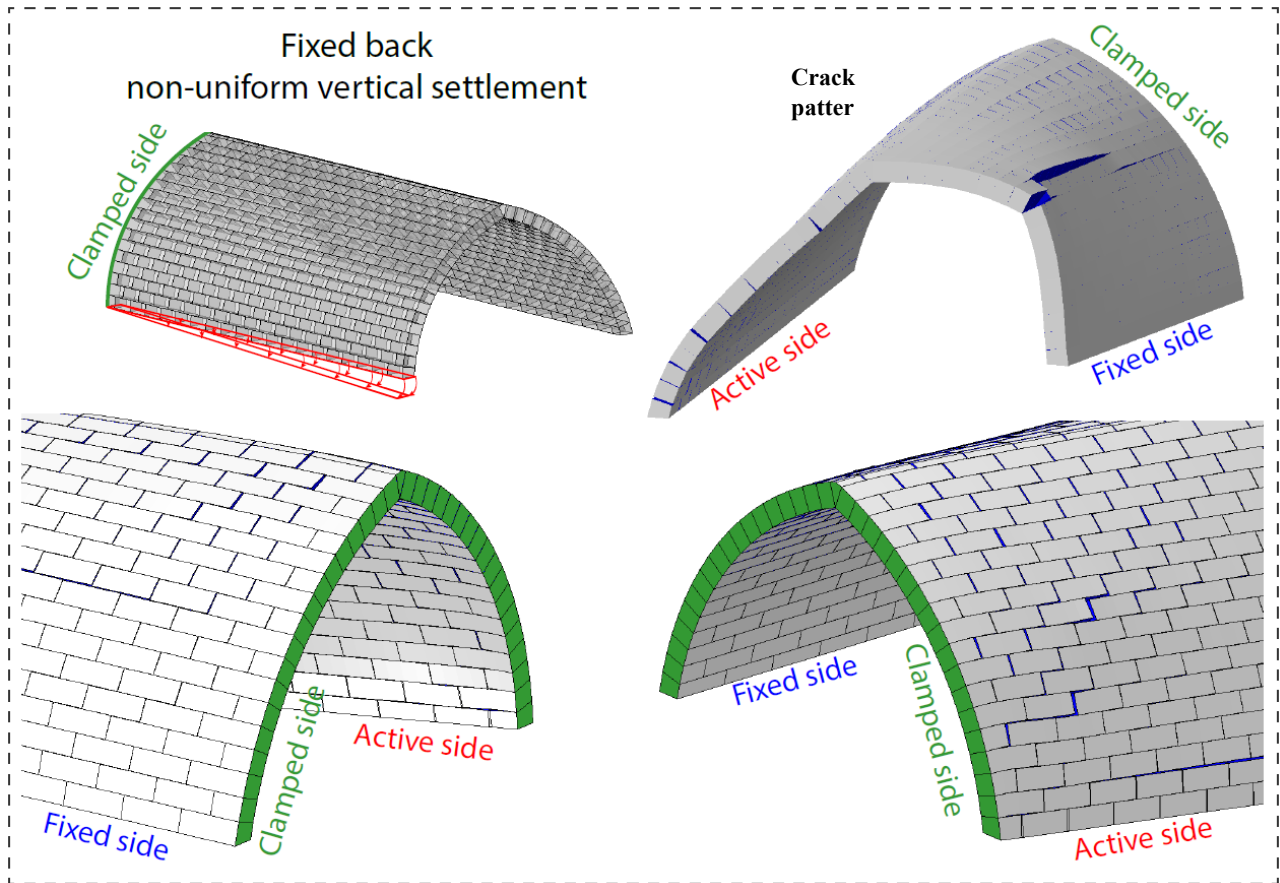


Fig. 9 – Fixed back non-uniform vertical settlement crack pattern.

## 6 Conclusions

In this paper, the effects of differential settlements on historic masonry barrel vaults have been investigated. A 3D non-standard contact-based model has been developed to reproduce experiments on a scaled pointed barrel vault specimen, representative of late medieval barrel vaults in Scotland, undergoing non-uniform differential settlement.

Firstly, there is good agreement between the experimental and numerical results in terms of crack pattern and transverses-longitudinal deformation profiles, capturing the major longitudinal cracks close to the applied settlement and also those at the other end of the vault.

Then, further analyses have been carried out to gain insight on the effects of several plausible uniform and non-uniform settlement patterns. All the failure modes have been collected according to the imposed settlement pattern. This summary of results, although preliminary, could help analysts in understanding the nature of the on-going deformation process in historic masonry vaults. The design of strengthening strategies can be made in the spirit of the “minimum intervention” principle to guarantee conservation is precise to the problems addressed or even considering not cancelling a deformation if it is proved to represent a significant phase or inherent design fault of the vault.

Further aspects, such as the influence of the nonlinear behaviour of the units, the dead load and the thickness of the vaults, the masonry bonding as also the segmentation of a vault (as masked by the ribs in Bothwell) should be investigated and collected in a more comprehensive matrix.

## Acknowledgements

Mauro Parodi, Massimo Damasio and Claudio Cavallero (<http://www.exemplar.com/>) are gratefully acknowledged for their technical support. Financial support by the Italian Ministry of Education, Universities and Research MIUR is gratefully acknowledged (PRIN2015 “Advanced mechanical modeling of new materials and structures for the solution of 2020 Horizon challenges” prot. 2015JW9NJT\_018).

## References

- [1] A. Romano and J. A. Ochsendorf, “The Mechanics of Gothic Masonry Arches,” *International Journal of Architectural Heritage*, vol. 4, no. 1, p. 59–82, 2010.
- [2] G. Ramaglia, G. P. Lignola and A. Prota, “Collapse analysis of slender masonry barrel vaults,” *Engineering Structures*, vol. 117, pp. 86–100, 2016.
- [3] A. M. D’Altri, G. Castellazzi, S. de Miranda and A. Tralli, “Seismic-Induced Damage in Historical Masonry Vaults: A Case-Study in the 2012 Emilia Earthquake-Stricken Area,” *Journal of Building Engineering*, vol. 13, p. 224–243, 2017 doi:10.1016/j.jobe.2017.08.005.
- [4] P. Block and J. Ochsendorf, “Thrust network analysis: A new methodology for three-dimensional equilibrium,” *Journal of the International Association for shell and spatial structures*, vol. 48, no. 3, pp. 167–173, 2007.
- [5] F. Fraternali, “A thrust network approach to the equilibrium problem of unreinforced masonry vaults via polyhedral stress functions,” *Mechanics Research Communications*, vol. 37, no. 2, p. 198–204, 2010.
- [6] F. Marmo and L. Rosati, “Reformulation and extension of the thrust network analysis,” *Computers & Structures*, vol. 182, p. 104–118, 2017.
- [7] P. Block and L. Lachauer, “Three-Dimensional (3D) Equilibrium Analysis of Gothic Masonry Vaults,” *International Journal of Architectural Heritage*, vol. 8, no. 3, p. 312–335, 2013.
- [8] H. Alexakis and N. Makris, “Hinging Mechanisms of Masonry Single-Nave Barrel Vaults Subjected to Lateral and Gravity Loads,” *Journal of Structural Engineering*, vol. 143, no. 6, 2017.
- [9] D. L. Fang, R. K. Napolitano, T. L. Michiels and S. M. Adriaenssens, “Assessing the stability of unreinforced masonry arches and vaults: a comparison of analytical and numerical strategies,” *International Journal of Architectural Heritage*, pp. 1–15, 2018.
- [10] E. Milani, G. Milani and A. Tralli, “Limit analysis of masonry vaults by means of curved shell finite elements and homogenization,” *International Journal of Solids and Structures*, vol. 45, no. 20, p. 5258–5288, 2008.
- [11] G. Milani, “Upper bound sequential linear programming mesh adaptation scheme for collapse analysis of masonry vaults,” *Advances in Engineering Software*, vol. 79, p. 91–110, 2015.

- [12] G. Creazza, R. Matteazzi, A. Sietta and R. Vitaliani, "Analyses of Masonry Vaults: A Macro Approach based on Three-Dimensional Damage Model," *Journal of Structural Engineering*, vol. 128, no. 5, p. 646–654, 2002.
- [13] G. Fortunato, M. F. Funari and P. Lonetti, "Survey and seismic vulnerability assessment of the Baptistery of San Giovanni in Tumba (Italy)," *Journal of Cultural Heritage*, vol. 26, pp. 64–78, 2017.
- [14] G. Barbieri, M. Valente, L. Biolzi, C. Togliani, L. Fregonese and G. Stanga, "An insight in the late Baroque architecture: An integrated approach for a unique Bibiena church," *Journal of Cultural Heritage*, vol. 23, p. 58–67, 2017.
- [15] G. Milani, M. Rossi, C. Calderini and S. Lagomarsino, "Tilting plane tests on a small-scale masonry cross vault: Experimental results and numerical simulations through a heterogeneous approach," *Engineering Structures*, vol. 123, p. 300–312, 2016.
- [16] D. Foti, V. Vacca and I. Facchini, "DEM modeling and experimental analysis of the static behavior of a dry-joints masonry cross vaults," *Construction and Building Materials*, vol. 170, p. 111–120, 2018.
- [17] G. Lengyel, "Discrete element analysis of gothic masonry vaults for self-weight and horizontal support displacement," *Engineering Structures*, vol. 148, p. 195–209, 2017.
- [18] I. Calì, F. Cannizzaro and M. Marletta, "A Discrete Element for Modeling Masonry Vaults," *Advanced Materials Research*, Vols. 133–134, p. 447–452, 2010.
- [19] B. Pantò, F. Cannizzaro, S. Caddemi, I. Calì, C. Chàcara and P. Lourenço, "Nonlinear Modelling of Curved Masonry Structures after Seismic Retrofit through FRP Reinforcing," *Buildings*, vol. 7, no. 79, 2017.
- [20] G. Lengyel and K. Bagi, "Numerical analysis of the mechanical role of the ribs in groin vaults," *Computers & Structures*, vol. 158, p. 42–60, 2015.
- [21] J. McInerney and M. J. DeJong, "Discrete Element Modeling of Groin Vault Displacement Capacity," *International Journal of Architectural Heritage*, vol. 9, no. 8, p. 1037–1049, 2014.
- [22] G. Lengyel and R. K. Németh, "The Mechanical Behavior of Ribs in Masonry Groin Vaults Subjected to Seismic Load," *International Journal of Architectural Heritage*, p. 1–15, 2018.
- [23] M. Gilbert and C. Melbourne, "Rigid-block analysis of masonry structures," *Structural engineer*, vol. 72, no. 21, 1994.
- [24] L. Cascini, R. Gagliardo and F. Portioli, "LiABlock\_3D: A software tool for collapse mechanism analysis of historic masonry structures," *International Journal of Architectural Heritage*, 2018 doi:10.1080/15583058.2018.1509155.
- [25] A. M. D'Altri, S. de Miranda, G. Castellazzi and V. Sarhosis, "A 3D Detailed Micro-Model for the In-Plane and Out-Of-Plane Numerical Analysis of Masonry Panels," *Computers & Structures*, vol. 206, pp. 18–30, 2018.

- [26] A. M. D'Altri, F. Messali, J. Rots, G. Castellazzi and S. de Miranda, "A damaging block-based model for the analysis of the cyclic behaviour of full-scale masonry structures," *Engineering Fracture Mechanics*, vol. 209, pp. 423-448, 2019.
- [27] J. Hudson and D. Theodossopoulos, "Gothic Barrel Vaults under Differential Settlement: The Effects of Boundary Conditions and FRP on Structural Behaviour," *Key Engineering Materials*, vol. 747, p. 496–503, 2017.
- [28] R. Fawcett, *Barrel-vaulted churches in late medieval Scotland, Architecture and Interpretation. Essays for Eric Fernie*, Boydell & Brewer: Martlesham, 2012.
- [29] D. Theodossopoulos, "Stone barrel vaulting in late medieval churches in Scotland," in *First Conference of the Construction History Society*, Cambridge, UK, 2014.
- [30] D. Theodossopoulos, N. Makoond and A. Lily, "The Effect of Boundary Conditions on the Behaviour of Pointed Masonry Barrel Vaults: Late Gothic Cases in Scotland," *The Open Construction and Building Technology Journal*, vol. 10, p. 274–292, 2016.
- [31] C. Carfagnini, S. Baraccani, S. Silvestri and D. Theodossopoulos, "The effects of in-plane shear displacements at the springings of Gothic cross vaults," *Construction and Building Materials*, vol. 186, p. 219–232, 2018.
- [32] *Abaqus®. Theory manual, Version 6.17, 2017.*
- [33] J. O. Hallquist, G. L. Goudreau and D. J. Benson, "Sliding interfaces with contact-impact in large-scale Lagrangian computations," *Computer Methods in Applied Mechanics and Engineering*, vol. 51, no. 1-3, p. 107–137, 1985.
- [34] P. B. Lourenço and J. G. Rots, "Multisurface Interface Model for Analysis of Masonry Structures," *Journal of Engineering Mechanics*, vol. 123, no. 7, p. 660–668, 1997.
- [35] R. van der Pluijm, "Shear behaviour of bed joints," in *6th North American Masonry Conference, 6-9 June 1993*, Philadelphia, Pennsylvania, USA, 1993.